Nucleosome Assembly on Telomeric Sequences†

Luigi Rossetti, Stefano Cacchione, Mario Fuà, and Maria Savino*

Istituto Pasteur Fondazione Cenci Bolognetti, Dipartimento di Genetica e Biologia Molecolare, Università di Roma "La Sapienza", P.le A. Moro 5, 00185 Roma, Italy

Received October 22, 1997; Revised Manuscript Received February 25, 1998

ABSTRACT: The organization of telomeric chromatin differs from that of bulk chromatin in some peculiar features, such as the unusually short nucleosomal spacing found in vertebrates. Telomeric DNAs are straight, since they consist mostly of 6−8-bp repeated sequences, therefore out of phase with the B DNA period. This feature should be of relevance in nucleosome formation, suggesting the usefulness of studying simple model systems of nucleosome assembly. We reconstituted nucleosomes in vitro, by using purified histone octamers and/or by octamer transfer from chicken erythrocyte nucleosomes, onto telomeric sequences from human, *Arabidopsis thaliana*, and *Saccharomyces cerevisiae*. All of these telomeres contain GGG and GGT triplets but are characterized by different repeat lengths (6, 7, and 8 bp). The free energies involved in the association process are the highest among the biological sequences so far assayed, suggesting a main role of DNA flexibility in the assembly of telomeric chromatin. Digestion studies with DNase I, hydroxyl radicals, exonuclease III, and λ exonuclease indicate that telomeric nucleosomes are characterized by multiple translational positioning without rotational phasing, whereas the telomeric DNA folding around the histone octamer shows the canonical periodicity of about 10.2 bp. The experimental results and a theoretical simulation of DNase I digestion indicate a multiple nucleosome positioning with the periodicity of telomeric DNA. This suggests a main role of local chemical recognition between telomeric sequences and the histone octamer in nucleosome assembly.

Telomeres,[1] the specialized structures located at the ends of eukaryotic chromosomes, are essential for chromosome stability and facilitate the complete replication of chromosomal termini (*1*, *2*). In most organisms telomeric DNA consists of a tandem array of short sequence motifs, typically containing tracts of three or four guanine bases on the 3′-ending strand. The conservation of this peculiar chemical feature in many different species argues for an important structural and functional role. Several investigations have shown that the telomeric G-rich strands can form DNA quadruplexes that may be involved in processes such as chromosome association (for a review, see refs *3* and *4*). More recently, telomeric C-rich strands were also found to be able to assume, in particular chemico-physical conditions, a folded secondary structure (*5*). Double-stranded telomeric sequences are recognized by proteins such as RAP1 in *Saccharomyces cerevisiae* or TRF in humans, forming specific complexes. A canonical B DNA conformation, although severely distorted in the middle of the binding site, emerges from the resolved structure of the RAP1 DNA binding domain (RAP1-DBD) bound to DNA (*6*). The particular characteristics of nearly all telomeric DNAs, namely the repeat length different from the B DNA double helical period and the presence of stretches of guanines only on one strand, do not seem to cause duplex structural features differing from average B DNA. However, these features could be of relevance when telomeric DNA is organized in nucleosomes.

The structure of rat liver telomeric chromatin has been recently characterized, revealing very regular arrays of closely packed nucleosomes with the unusually short repeat length of 157 bp (*7*). Repeat lengths shorter than bulk chromatin have been found in telomeres of several other eukaryotes (*8*−*10*). More recently, Bedoyan et al. (*11*) showed that a major fraction of rat liver telomeric nucleosomes can condense into higher-order structures only slightly different from those of bulk chromatin, suggesting a more compact structure of telomeric chromatin. The linker histone H1 binds to telomeres, probably less strongly than to bulk chromatin due to the shorter linker (*11*). In contrast to this, Muyldermans et al. (*12*) found the same spacing in telomeric and bulk chromatin from chicken erythrocytes; furthermore, in chicken erythrocytes linker histones H1 and H5 appear able to discriminate between telomeric and bulk nucleosomes. Finally, telomeric chromatin seems to be hypersensitive to micrococcal nuclease digestion (*7*, *8*, *10*); this finding has been tentatively attributed to the increased sliding mobility of telomeric nucleosomes and/or to the interactions with specific telomeric proteins. These results strongly suggest the usefulness of studying telomeric nucleosomes by in vitro approaches, using simple model systems consisting only of telomeric DNA and purified histone octamer.

In wrapping around the histone octamer, DNA must be dramatically curved. DNA curvature and/or curvability is one of the main determinants of its affinity for the histone

† This work was partially supported by cofin.MURST 97 CFSIB.

* Corresponding author. Tel: (39)-6-49912238. Fax: (39)-6-4440812. E-mail: m.savino@caspur.it.

[1] Abbreviations: bp, base pair(s); DBD, DNA binding domain; EDTA, ethylenediaminetetraacetic acid; PMSF, phenylmethanesulfonyl fluoride; PCR, polymerase chain reaction; SDS, sodium dodecyl sulphate; DNase I, deoxyribonuclease I; Exo III, exonuclease III.

S0006-2960(97)02618-4 CCC: $15.00
Published on Web 04/28/1998

octamer and regulates rotational and translational nucleosome positioning on different sequences (*13*). The rotational orientation of DNA relative to the histone octamer surface is principally determined by the periodic occurrence of short sequence motifs in phase with the DNA helical repeat (*13*−*15*), such as A/T-rich sequences that preferentially occur when the minor groove points in toward the histone octamer. Telomeric repeats, in most cases 6−8 bp long, are out of phase with the DNA helical period on the nucleosome (10.2 bp). This feature could have two consequences: a higher free energy of nucleosome formation on telomeres compared with average sequences and multiple nucleosome positioning without rotational phase. We have recently obtained support for the first part of this hypothesis, since telomeric sequences from different eukaryotic groups show significantly lower association constants with the histone octamer than average DNA (*16*). These findings suggest that the folding of telomeric sequences around the histone octamer and the translational positioning of telomeric nucleosomes could be different from bulk DNA and prompted us to further investigate these features. Moreover, DNA chemical determinants could be particularly relevant to nucleosome multiple translational positioning in the case of repetitive sequences (*15*, *17*), since several virtual nucleosome positions span the same sequence, characterized by equal curvature and chemical interactions. Therefore, studying nucleosome positioning along telomeric sequences seems of interest both to elucidate the structural features of telomeric chromatin and to obtain information on the role of chemical determinants in nucleosome assembly.

MATERIALS AND METHODS

DNA Fragments. Synthesis, multimerization, and cloning of telomeric sequences from human, $(GGGTTA)_{28}$, *Arabidopsis thaliana*, $(GGGTTTA)_{24}$ and $(GGGTTTA)_{34}$, and *S. cerevisiae*, $(GGTGTGTG)_{20}$, were performed as previously described (*16*). Plasmid pXbsF201, carrying the 249-bp *Xenopus borealis* somatic 5S RNA gene inserted in the *Hin*dIII-*Bam*HI site of pUC9 (*18*) was a gift of I. Ruberti. For DNase I, hydroxyl radical, Exo III, and λ exonuclease experiments, DNA fragments were radiolabeled only on one strand. Plasmids containing the telomeric sequences were linearized with a first restriction enzyme (*Eco*RI or *Bam*HI), 3′-end-labeled by filling in with [α-^{32}P]dATP and Klenow enzyme or 5′-end-labeled with [γ-^{32}P]ATP and T4 polynucleotide kinase, and finally digested with a secondary restriction enzyme (*Bam*HI or *Eco*RI, *Hin*dIII for pXbsF201). The labeled fragments were then recovered from preparative polyacrylamide gel. Internally labeled DNAs were obtained by 30-cycle PCR amplification in the presence of [α-^{32}P]-dCTP. A 19-mer (TTGGGAAACAGCTATGACCAT) and a 21-mer (ACAGGAAACAGCTATGACCAT), which hybridize outside of the polylinker region of pUC18, were used as primers. Amplification products were then digested with *Eco*RI and *Bam*HI and purified on a 5% native polyacrylamide gel.

Electrophoretic Mobility Assay. End-labeled DNA fragments were run on a native 8% polyacrylamide gel (40 × 20 × 0.75 cm) in 1X TBE buffer (90 mM Tris-Borate, 2 mM EDTA, pH 8.3) at a constant voltage of 4 V/cm. Gels were dried and autoradiographed; the electrophoretic mobility of the samples was then compared with that of a molecular weight standard.

Nucleosome Reconstitution and Gradient Purification. Nucleosome reconstitution was carried out either by octamer transfer (*19*, *20*) or by adding purified histone octamers (*20*) with minor modifications. Briefly, about 30 ng of end-labeled DNA ((1−2) × 10^6 cpm) was mixed with 2 μg H1- and H5-depleted oligonucleosomes obtained from chicken erythrocytes (*16*) in 1 M NaCl, 10 mM Tris-HCl pH 8, 1 mM EDTA pH 8, 0.1 mM PMSF, 0.1% Nonidet P-40, in a final volume of 20 μL. After 30 min of incubation at room temperature, samples were diluted to 100 mM NaCl with serial additions of 10 mM Tris-HCl pH 8, 1 mM EDTA pH 8, 0.1 mM PMSF, 0.1% Nonidet P-40 (3, 7, 10, 40, and 120 μL, 10 min apart, room temperature). Alternatively, radiolabeled DNA was mixed with 2 μg of core histones prepared from chicken erythrocytes (*21*) and 2 μg of nucleosomal DNA as a competitor, in 2 M NaCl, 10 mM Tris-HCl pH 8, 1 mM EDTA pH 8, 0.1 mM PMSF, 0.1% Nonidet P-40, in a final volume of 10 μL. After incubation at room temperature for 30 min, the salt concentration was lowered to 100 mM with several additions of different volumes of 10 mM Tris-HCl pH 8, 1 mM EDTA pH 8, 0.1 mM PMSF, 0.1% Nonidet P-40. The sample was then loaded at the top of a 5-mL gradient of 5−25% sucrose containing 10 mM Tris-HCl pH 8, 1 mM EDTA pH 8, 0.1 mM PMSF, 0.1% Nonidet P-40 and centrifuged for 18 h at 40 000 rpm in a SW50-1 rotor at 4 °C. Fractions (150 μL) were collected from the bottom of the gradient and counted in a scintillation counter to identify the free DNA and nucleosome peaks (Figure 1, left). Aliquots (5 μL) of each fraction were also electrophoresed on a native 4% acrylamide 0.5 X TBE gel (0.45 M Tris-borate, 1 mM EDTA, pH 8.3) for 3 h at 200 V, so that the fractions containing the reconstituted nucleosomes were identified by their mobility (Figure 1, right), pooled, dialyzed against TE, and stored at 4 °C.

DNase I Footprinting Assay. Footprinting of reconstituted nucleosomes was performed in parallel with free DNA samples dissolved in the same final buffer. To avoid misinterpretations due to the presence of free DNA in the nucleosome samples, nuclease and hydroxyl radical digestions were performed with either of the following two methods. In the first, gradient-purified nucleosomes (see the description above) were used. In the second procedure, samples were cleaved with the appropriate probe and run on a preparative 1% agarose gel, and the nucleosome band was excised and purified. Both methods gave similar results in all footprinting assays.

After the addition of $MgCl_2$ to a final concentration of 5 mM, samples were treated for 1 min at 25 °C with 0.2−1 U/mL (free DNA) or 2−10 U/mL DNase I (nucleosome) in a 50 μL total volume. When internally labeled DNA was used, DNase I final concentrations were 10−100 U/mL (free DNA) and 50−500 U/mL (nucleosome). Reactions were stopped by adding 50 μL of 20 mM EDTA. Samples were then phenol extracted, ethanol precipitated, and run onto 6% polyacrylamide−urea sequencing gels, containing 30% formamide. Gels were fixed in 20% methanol and 5% acetic acid, dried, and autoradiographed. Autoradiographs were scanned with a BioRad GS-670 imaging densitometer.

Hydroxyl Radical Footprinting Assay. Hydroxyl radical cleavage was performed essentially according to Tullius et

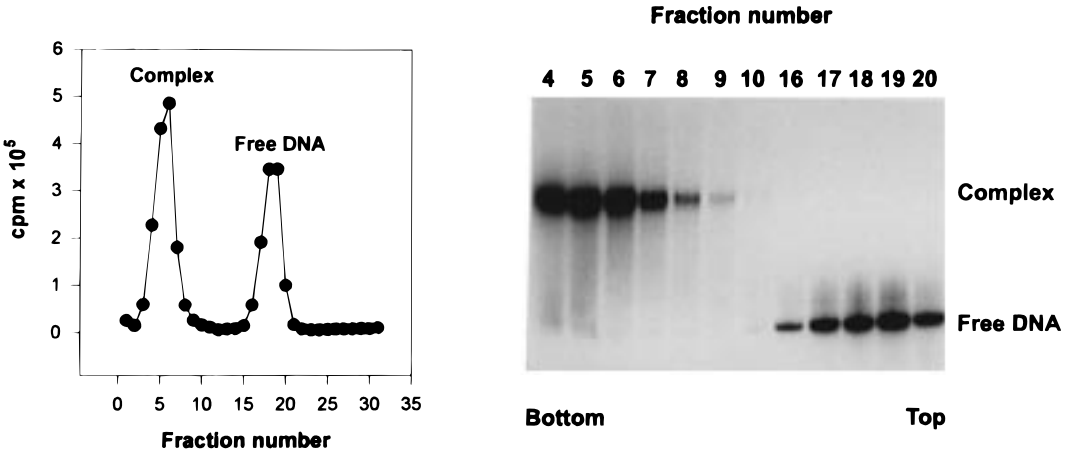

FIGURE 1: Purification of reconstituted nucleosomes. Left: fractionation on sucrose gradients of telomeric DNA reconstituted with purified histone octamer. Gradient fractionation is monitored by liquid scintillation counting, with the first fraction coming from the bottom of the gradient. Right: aliquots (5 μL) of each fraction analyzed on a native 5% polyacrylamide gel to visualize contamination of nucleosome fractions with free DNA.

al. (*22*). Sodium ascorbate, hydrogen peroxide, $(NH_4)_2Fe(SO_4)_2$, and EDTA (final concentration 1 mM, 0.03%, 50 mM, and 100 mM, respectively) were added in a total volume of 80 μL. The final concentrations of the reagents were 10-fold lower in the case of free DNA. Reactions were stopped after 1−4 min at room temperature by adding an equal volume of 140 mM thiourea, 140 mM EDTA. Samples were then extracted with phenol and precipitated with ethanol. Separation on 6% sequencing gels and subsequent fixing, drying, and exposure were as described above.

Exonuclease III and λ Exonuclease Footprinting Assays. Reconstituted nucleosomes, labeled on the 5′ end, were made (66 mM Tris-HCl (pH 8), 1.66 mM $MgCl_2$, 1 mM 2-mercaptoethanol) and digested at 37 °C with Exo III (final concentration 80 U/mL); samples were withdrawn at appropriate intervals, and the reaction was stopped by adding an equal volume of 20 mM EDTA, 1% (w/v) SDS and heating at 70 °C for 5 min. For the λ exonuclease cleavage reactions, nucleosomes reconstituted onto 3′-labeled DNA were used. Samples were made (5 mM $MgCl_2$) and digested with λ exonuclease (final concentration 30 U/mL) for 20−40 min at 37 °C. The reaction was stopped with an equal volume of 20 mM EDTA, 0.2% SDS. Samples were phenol extracted and analyzed on 6% denaturing polyacrylamide gels. Gel analysis was as described above.

RESULTS

Stability and Positioning of Telomeric Nucleosomes: DNase I and Hydroxyl Radical Footprintings Reveal Multiple Nucleosome Translational Positioning without Rotational Phasing. A histone octamer can assemble virtually with all DNA sequences, but the stability of nucleosomes can vary widely (*23*−*25*). We have recently shown that the telomeric sequences from *S. cerevisiae*, human, and *Arabidopsis* form nucleosomes with lower affinities than average sequences (*16*). Since DNA curvature and/or flexibility are important in determining nucleosome formation and stability (*23*, *26*), we analyzed the mobilities of telomeric DNAs on polyacrylamide gels, a useful tool for characterizing DNA superstructural features (*27*−*29*). The mobilities of yeast (170 bp), human (190 bp), and *Arabidopsis* (190 bp) telomeric DNAs on an 8% native polyacrylamide gel run at room temperature appear to be in agreement with their molecular weights (not shown). In fact the ratios between apparent and real molecular weight are 1.05 ± 0.05 in all cases; this quite normal electrophoretic mobility is typical of globally straight DNA.

Table 1: Comparative Free Energies in Nucleosome Formation Expressed Relative to Average Sequence Nucleosomal DNA

DNA	ΔΔ*G* (kcal/mol)
Saccharomyces cerevisiae telomere[a] $(GGTGTGTG)_{20}$	1.60
human telomere[a] $(GGGTTA)_{28}$	1.35
Arabidopsis thaliana telomere[a] $(GGGTTTA)_{24}$	1.10
mononucleosomal DNA	0.00
Xenopus borealis somatic 5S rRNA gene[b]	−1.75
$(CTG)^{62}$ [b]	−2.80
TG-pentamer[c]	−2.85
TATA-repeat sequences[d]	∼−3.00/−3.30
histone H4 gene[b]	−3.21

[a] Reference 16. [b] Reference 42. [c] Reference 23. [d] Reference 25. In the original paper free energy values are reported in kJ/mol.

To study nucleosome positioning on the telomeric sequences reported in Table 1, we have used different enzymatic and chemical probes. DNase I footprinting is well-known to provide information on the helical periodicity of DNA−protein interactions (*19*). Favored positions of cleavage within the nucleosome core DNA lie at intervals of about 10 nucleotides, corresponding to the points where the minor groove faces outward. When a DNA sequence is rotationally positioned with respect to the histone octamer, the same face of DNA will always be exposed on the outside; therefore DNase I cleavage will generate a 10-bp ladder. DNAs without a preferred rotational positioning or with several alternative frames of rotational positioning will not show a clear 10-bp cleavage periodicity or even lack a nucleosome-specific DNase I pattern. The DNase I footprintings reported in Figure 2 show some features that are common to the three telomeres. Both in free DNA and in nucleosome, a cutting periodicity equal to the telomeric repeat length was found, reasonably depending on DNase I sequence specificity (*30*). An underlying periodicity of about 10 bp is not detectable in the nucleosomal pattern, indicating the absence of a rotational setting. In all cases the central

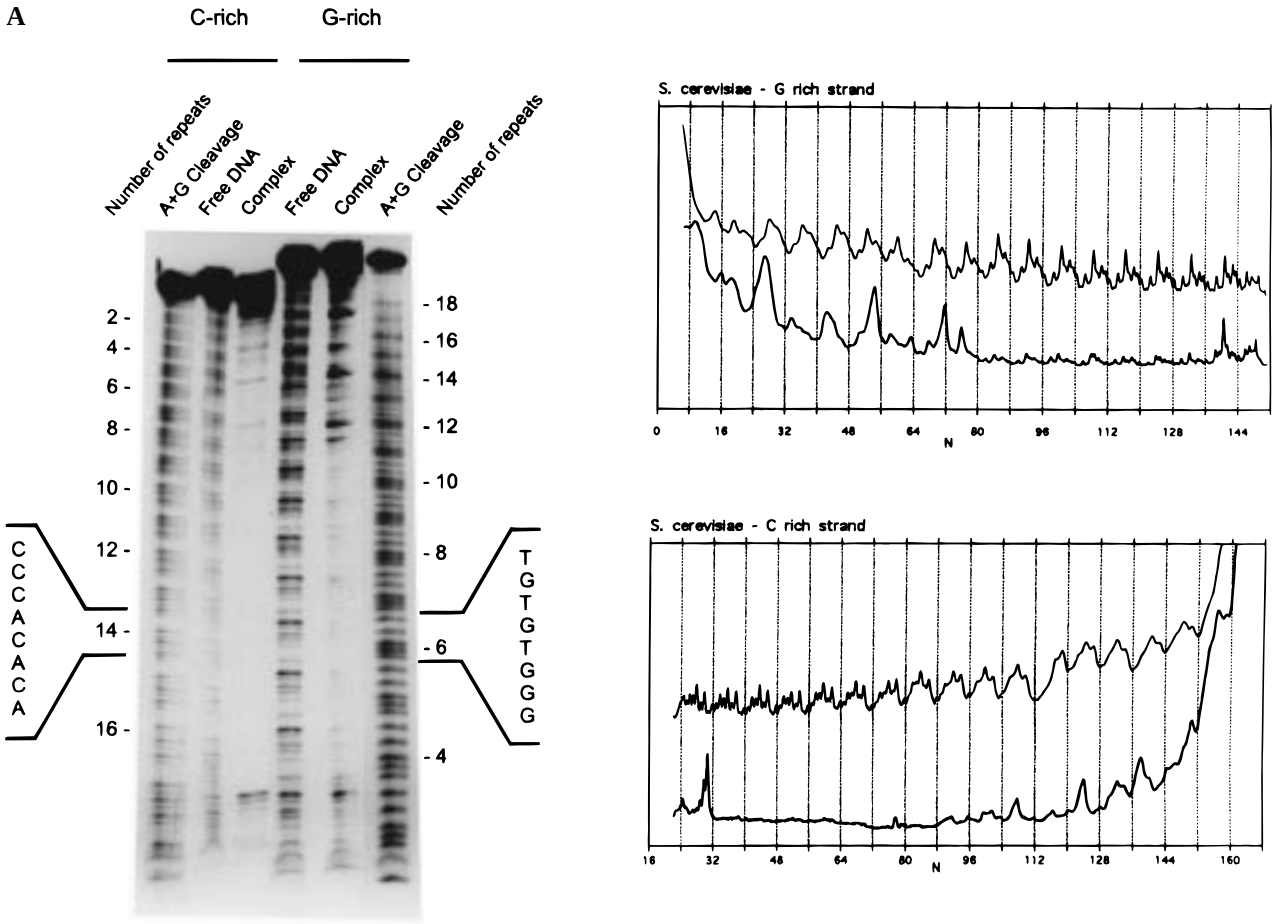
A
C-rich
G-rich
Number of repeats
A+G Cleavage
Free DNA
Complex
Free DNA
Complex
A+G Cleavage
Number of repeats
2 -
4 -
6 -
8 -
10 -
12 -
14 -
16 -
- 18
- 16
- 14
- 12
- 10
- 8
- 6
- 4
CCCACACA
TGTGTGGG
S. cerevisiae - G rich strand
0 16 32 48 64 80 96 112 128 144
N
S. cerevisiae - C rich strand
16 32 48 64 80 96 112 128 144 160
N

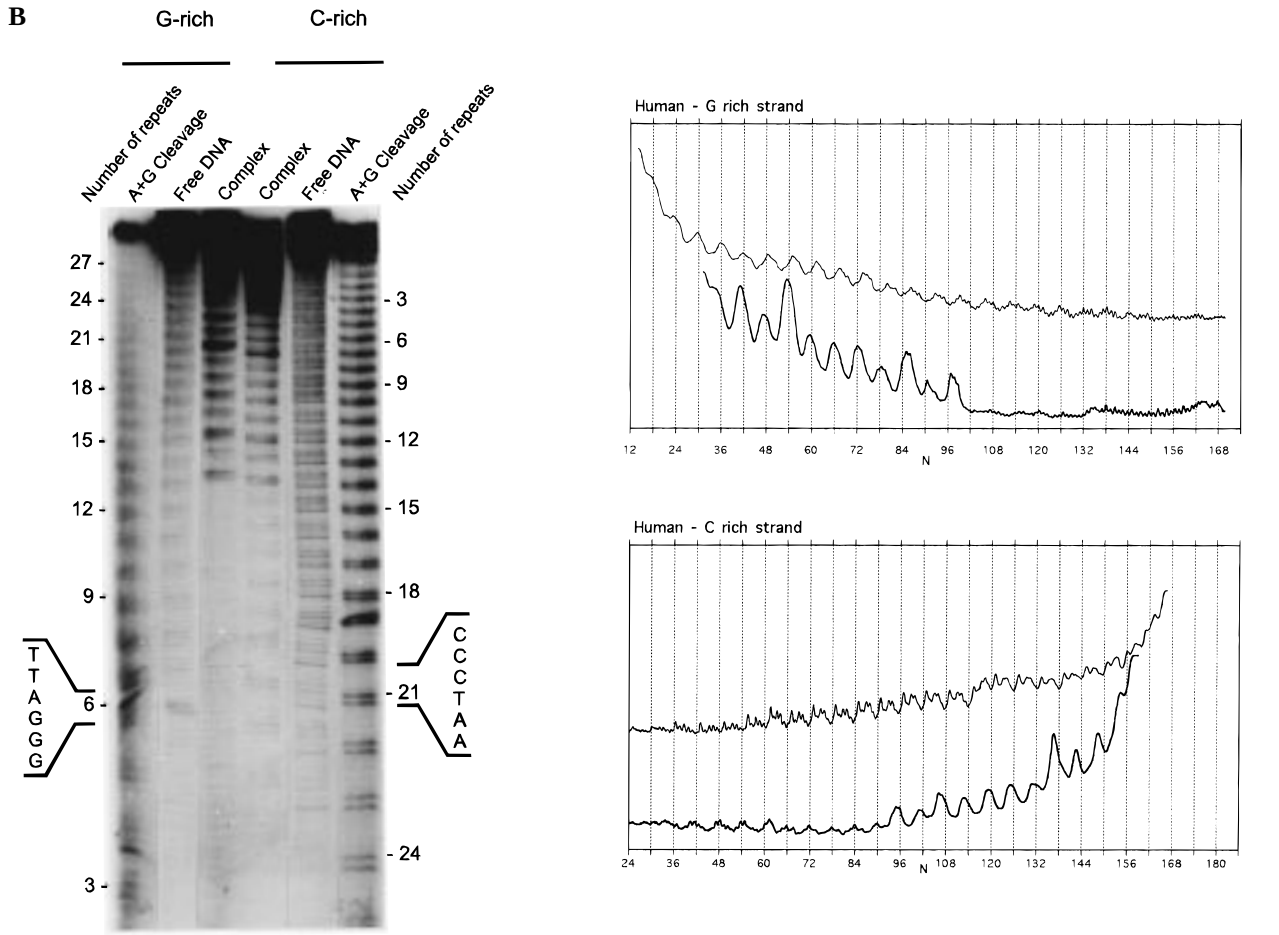
B
G-rich
C-rich
Number of repeats
A+G Cleavage
Free DNA
Complex
Complex
Free DNA
A+G Cleavage
Number of repeats
27 -
24 -
21 -
18 -
15 -
12 -
9 -
6 -
3 -
- 3
- 6
- 9
- 12
- 15
- 18
- 21
- 24
TTAGGG
CCCTAA
Human - G rich strand
12 24 36 48 60 72 84 96 108 120 132 144 156 168
N
Human - C rich strand
24 36 48 60 72 84 96 108 120 132 144 156 168 180
N

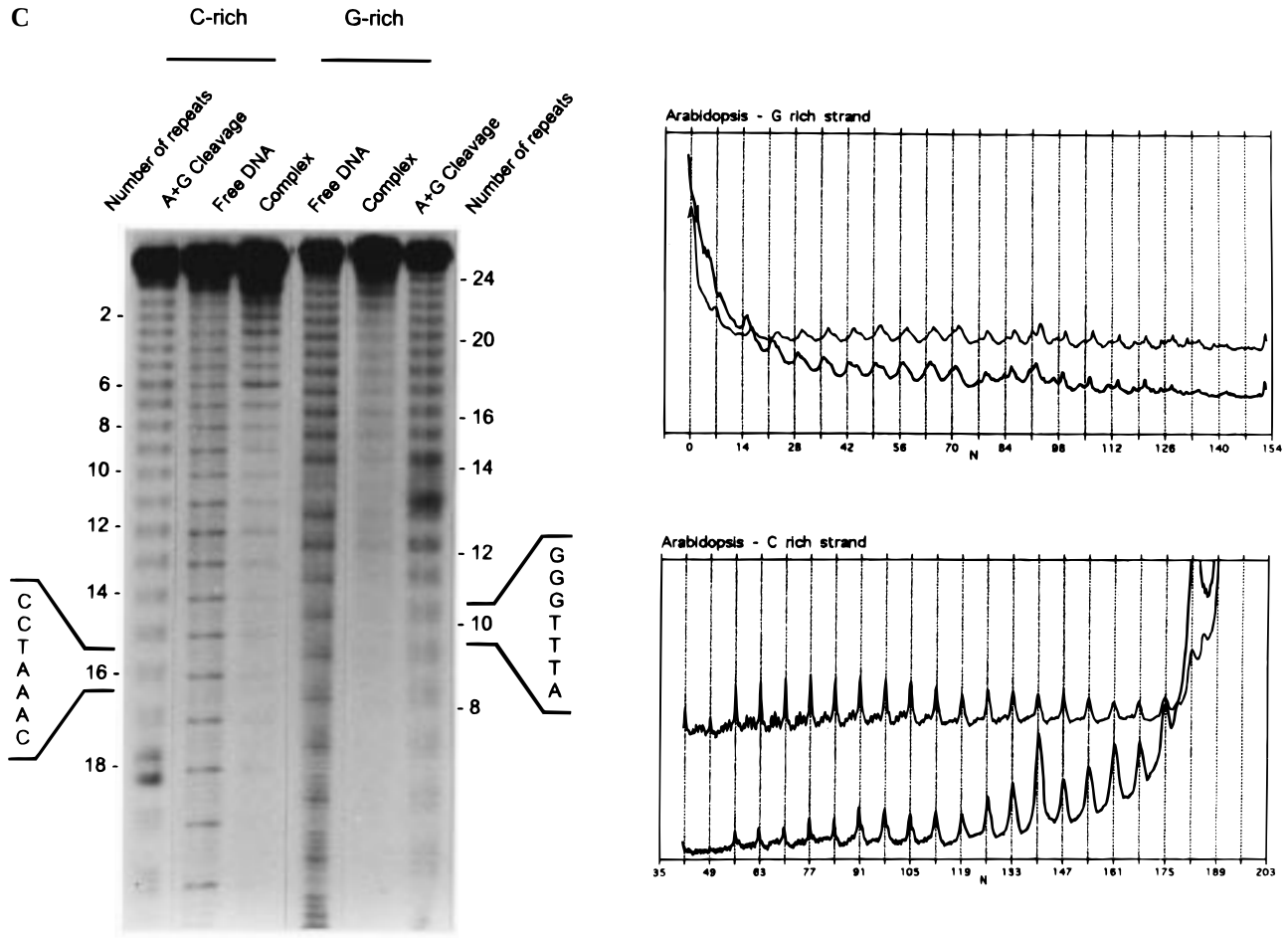

FIGURE 2: DNase I footprinting of nucleosome reconstituted onto telomeric DNAs from (A) *S. cerevisiae*, (B) human, (C) *Arabidopsis*. Left: footprints of G-rich and C-rich strands labeled on the 3′ end. A + G is a Maxam−Gilbert sequencing reaction for purines. The DNA length has been indicated as the number of telomeric repeats starting from the 5′ end of the G-rich strand. Right: densitometric profiles of the reported footprints. In each panel the upper profile refers to free DNA and the lower profile to the nucleosome complex.

region of the fragment is depressed in the nucleosome compared with the free DNA pattern. These features suggest multiple nucleosome positioning without rotational phase on telomeric sequences, a result expected considering that the repeat lengths of telomeres are out of phase with DNA helical periodicity on the nucleosome. However, a surprising feature of the DNase I cleavage patterns on the nucleosome is the presence of a set of remarkably intense bands in the range of high molecular weights. The periodicity of these bands is equal to the telomeric repeats in human and *Arabidopsis* (Figure 2B,C), while in the case of yeast telomere (Figure 2A), it corresponds to multiples of the telomere repeat. This unusual feature can be reasonably attributed to the peculiarity of telomeric sequences and will be interpreted in the next section.

Since DNase I digestion patterns have revealed a strong sequence-dependent cleavage specificity (*30*), we carried out similar digestion experiments using hydroxyl radicals (*22*). The small size and the low sequence specificity of the hydroxyl radicals compared with DNase I make this probe a widespread tool to measure DNA periodicity on the nucleosome (*26*). Figure 3 shows hydroxyl radical footprinting of nucleosomes reconstituted onto yeast telomeric DNA. The hydroxyl radical cleavage of the *X. borealis* 5S RNA gene, reported as an example of a reconstituted positioned nucleosome (*26*), clearly shows the 10-bp periodicity of nucleosomal DNA. On the contrary, the free DNA and the nucleosome patterns of yeast telomeres are almost indistinguishable; both present an 8-bp periodicity, slightly more evident in the nucleosomal pattern. Also this probe fails to reveal a 10-bp periodicity in the reconstituted nucleosome cleavage pattern, confirming the lack of nucleosome rotational phasing shown by DNase I analyses. Similar results have been obtained for *Arabidopsis* and human telomeric sequences (not shown). The presence of a periodicity correlated to the sequence repeat length is probably due to the capability of the hydroxyl radical to reveal structural details of DNA (*31*). Sequence specificity of the hydroxyl radical cutting is also possible (*32*), although in the experimental conditions used, this reagent attacks the deoxyribose and not the bases (*22*, *31*).

Theoretical Simulation of DNase I Cleavage Patterns of Telomeric Nucleosomes Indicates Multiple Nucleosome Positioning with a Spacing Equal to the Telomeric DNA Repeats. To give a better interpretation of the experimental data, we compared them with the expected DNase I patterns obtained from a theoretical simulation that we carried out on the basis of the following assumptions:

(1) The pseudo-dyad axis of the histone octamer always faces the major groove of the DNA double helix (*33*); that is, its rotational phase is defined implicitly by its translational position.

(2) The effect of the nucleosome on the DNase I activity is a modulation of the probability of cleavage which varies

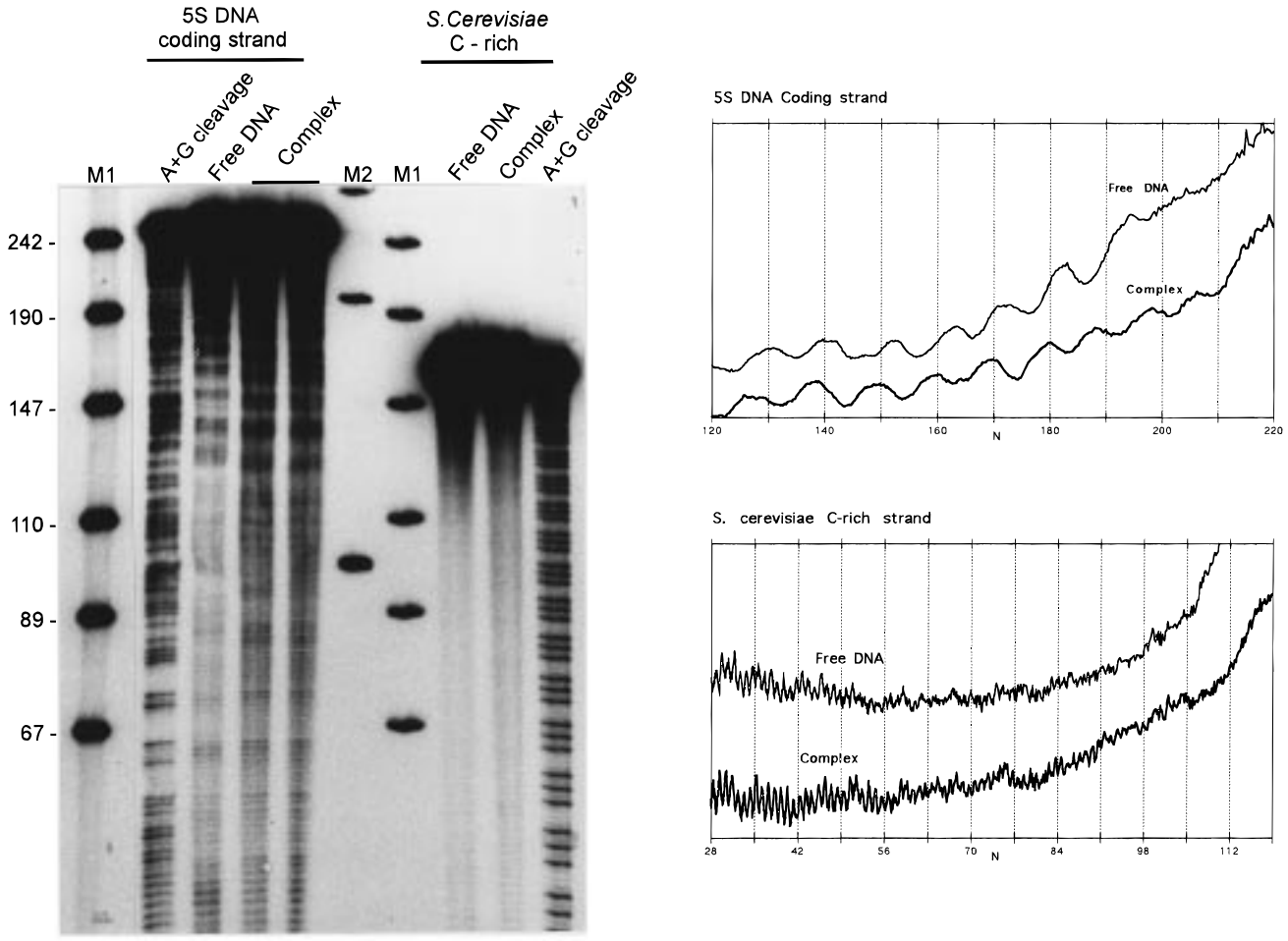

FIGURE 3: Left: hydroxyl radical footprinting of the 5S RNA gene coding strand and the yeast telomeric DNA C-rich strand, labeled on the 3′ end. A + G is a Maxam−Gilbert sequencing reaction for purines. M1 is a digest of pUC18 with *Hpa*II, and M2 is a 100-bp DNA ladder (Pharmacia). Right: densitometric profiles of the reported footprints; free DNA (upper profile), nucleosome complex (lower profile).

in different regions of the DNA tract complexed with the histone octamer. This was extensively studied by Lutter (*34*), and we referred to his paper in order to obtain the trend of the probability of cleavage for the region of DNA involved in the complex. His experimental histogram was transformed in a continuous function (LF(s)) by convolving it with a Gaussian, and then normalized. As discussed by Lutter, this function is not symmetric (specular) with respect to the central position but is polar along one strand. The author shows that the asymmetry is compatible with the existence of a dyad axis in the nucleosome structure and suggests that it could be in relation to the path of the nucleosome superhelix.

(3) Two alternative hypotheses were made concerning the translations of the nucleosome along the telomeric sequence: (a) chemical recognition does not play a role in nucleosome positioning and therefore each translational position is almost equally probable; and (b) there is some kind of sequence recognition. In this case there are p (p is the telomeric repeat) nonequivalent translational positions and one is preferred over the others; equivalent nucleosome positions are separated by a number of base pairs equal to the repeat of the telomere.

DNase I has a sequence specificity that was extracted from the experimental free DNA degradation pattern. The probability of cleavage as a function of the sequence position for free DNA ($Pf(s)$) is a periodic function with period p. According to the preceding hypotheses, the probability of cleavage for a DNA tract that forms a nucleosome with its dyad axis at the sequence position s_o ($PN(s,s_o)$) can be estimated as

$$PN(s,s_o) = (Pf(s)LF(s - (s_o - 72))$$

when $(s_o - 72) < s < (s_o + 72)$, otherwise:

$$PN(s, s_o) = Pf(s)$$

Since the DNA is labeled at one end, the probability (P_{lab}-(s,s_o)) of obtaining from this DNA tract a labeled fragment of length s is the combined probability of having a cleavage at position s and not having a cleavage at any of the positions preceding s:

$$P_{lab}(s, s_o) = PN(s, s_o) \prod_{j=1}^{s-1} (1 - PN(j, s_o))$$

This probability has to be evaluated for all the possible values of s_o (i.e., for all the possible positions of the nucleosome along the DNA tract) and summed up to give a number which is proportional to the observed optical density of the

electrophoretic band at position *s* (OD(*s*)). Considering as in hypothesis a each translational position equally probable:

$$\mathrm{OD(s)} \propto \sum_{s_o=72}^{n-72} P_{\mathrm{lab}}(s, s_o)$$

where *n* is the length in base pairs of the DNA tract.

On the contrary, considering only one of the *p* positions strongly preferred over the others (hypothesis b), the summation simply runs in steps of *p* bases along the sequence.

According to these assumptions, we have obtained theoretical DNase I digestion patterns in the case of the three telomeric nucleosomes studied experimentally. The simulation was carried out in the two cases of translational positions differing by one or *p* base pairs. All of the theoretical patterns obtained contain a central depressed region in agreement with the experiments (Figure 4); therefore this feature does not allow the discrimination between the two different models of nucleosome positioning.

More informative is another feature emerging from the experimental digestion patterns, namely, the series of particularly intense periodical bands; this feature is better reproduced in the theoretical pattern under the hypothesis that the translational positioning of the nucleosome depends on the periodicity of the telomeres and that the possible positions differ by multiples of *p* bp (lower profiles, hypothesis b). The patterns obtained simulating translational positions differing by 1 bp (upper profiles, hypothesis a) are smoother, not accounting for the presence of the characteristic strong bands visible in the experimental patterns. Thus, the comparison between simulated (Figure 4) and experimental (Figure 2) digestion patterns gives a strong indication that the more suitable model of nucleosome positioning is that outlined in hypothesis b, namely, that the multiple nucleosome positions have a spacing equal to *p*, where *p* is the telomeric sequence repeat.

In the case of human and *Arabidopsis* telomeres, the agreement between theoretical and experimental patterns is quantitative considering both the relative intensities and the positions of the bands; in the case of yeast, the experimental bands show a superperiodicity, which deserves further investigations. The simulation allows us to interpret the rather complex experimental patterns as a self-convolution of the Lutter cleavage pattern over the multiple nucleosome positions. This indirectly means that the structure and periodicity of telomeric nucleosomes are the same as those of bulk nucleosomes because the DNase I cleavage pattern as discussed by Lutter is sensitive to the details of the nucleosome structure.

The Helical Periodicity of DNA in Telomeric Nucleosomes is That of Nucleosomal DNA. The satisfactory agreement between experimental and theoretical DNase I digestion patterns indicates that the helical periodicity of DNA in nucleosomes assembled on telomeric sequences should correspond to that of the canonical conformation. Nevertheless, the relevance of this parameter to the structural features of telomeric nucleosomes prompted us to carry out direct measurements. This was made reconstituting nucleosomes on internally labeled telomeric DNA. Telomeric nucleosomes were treated with increasing amounts of DNase I in order to completely digest the DNA tails external to the nucleosome core allowing the 10-bp cleavage pattern of DNase I on the nucleosome to emerge. Figure 5 shows DNase I footprinting on nucleosomes reconstituted onto internally labeled *Arabidopsis* telomeric DNA. When low DNase I amounts are used (Figure 5, lane 4), undigested DNA is still present and the 7-bp sequence-specific periodicity is predominant; at higher DNase I concentrations, undigested DNA disappears and the 10-bp cleavage pattern of nucleosomal core DNA becomes evident (Figure 5, lanes 5 and 6). From the densitometric profiles it is possible to derive, via Fourier Transform, that while at beginning the periodicity is equal to the telomeric repeat (7 bp), in the progression of enzyme action the periodicity of the cleavage becomes equal to that of nucleosomal DNA, 10.2 ± 0.2 bp. Similar results have been obtained from prolonged DNase I digestion of nucleosomes reconstituted onto yeast and human telomeric sequences (not shown).

Exonuclease III and λ Exonuclease Digestion Patterns are Consistent with Nucleosome Multiple Positioning Having a Spacing Equal to the Telomeric Repeat. Exo III digests processively double-stranded DNA from the 3′-end. The progression of the enzyme is blocked by the borders of the histone octamer complex. Therefore, in controlled experimental conditions (*35*, *36*), Exo III allows the identification of nucleosome translational positions.

Figure 6A shows Exo III digestion patterns of a 240-bp *Arabidopsis* telomeric DNA. A striking feature of Exo III activity on telomeric DNA is the dramatically different reactivity of the two strands; free DNA is completely digested on the C-rich strand, whereas the G-rich strand shows sequence-specific bands even at high enzyme concentration (*37*). Exo III nucleosomal digestion patterns show a periodicity practically equal to the telomeric repeat length (Figure 6A). Even if the sequence-dependent Exo III cutting on the G-rich strand does not allow one to easily distinguish sequence-specific from nucleosomal borders stops, the distances between the stops on the two strands are mainly in the range 146 ± 2 bp corresponding to "bona fide" nucleosomes. Exo III analyses on human and yeast telomeric sequences give similar results (not shown).

However, to overcome the problem of Exo III sequence specificity, we used a different probe, λ exonuclease, to map the borders of telomeric nucleosomes. λ exonuclease degrades double-stranded DNA starting from the 5′ end of the molecule. The rate of digestion by λ exonuclease is highly processive and independent of DNA base composition (*38*). This enzyme has been used to map the binding sites of transcription factors (*39*, *40*); moreover, mapping of nucleosome positions with λ exonuclease is consistent with site-directed hydroxyl radical mapping (*41*) and Exo III footprinting (R. Negri and M. Buttinelli, personal communication). Figure 6B shows a λ exonuclease footprinting of a 240-bp *Arabidopsis* telomeric DNA. Free DNA is completely digested, whereas the nucleosomal cleavage pattern is characterized by bands spaced every 7 bp, the length of an *Arabidopsis* telomere repeat. The nucleosome borders identified on the C-rich strands correspond to the nucleosome borders found on the G-rich strand that are 146 ± 2 bp away. These nucleosome positions have been numbered on Figure 6B. Both types of exonuclease analyses are consistent with DNAse I footprinting and the theoretical simulation and are a strong support to multiple

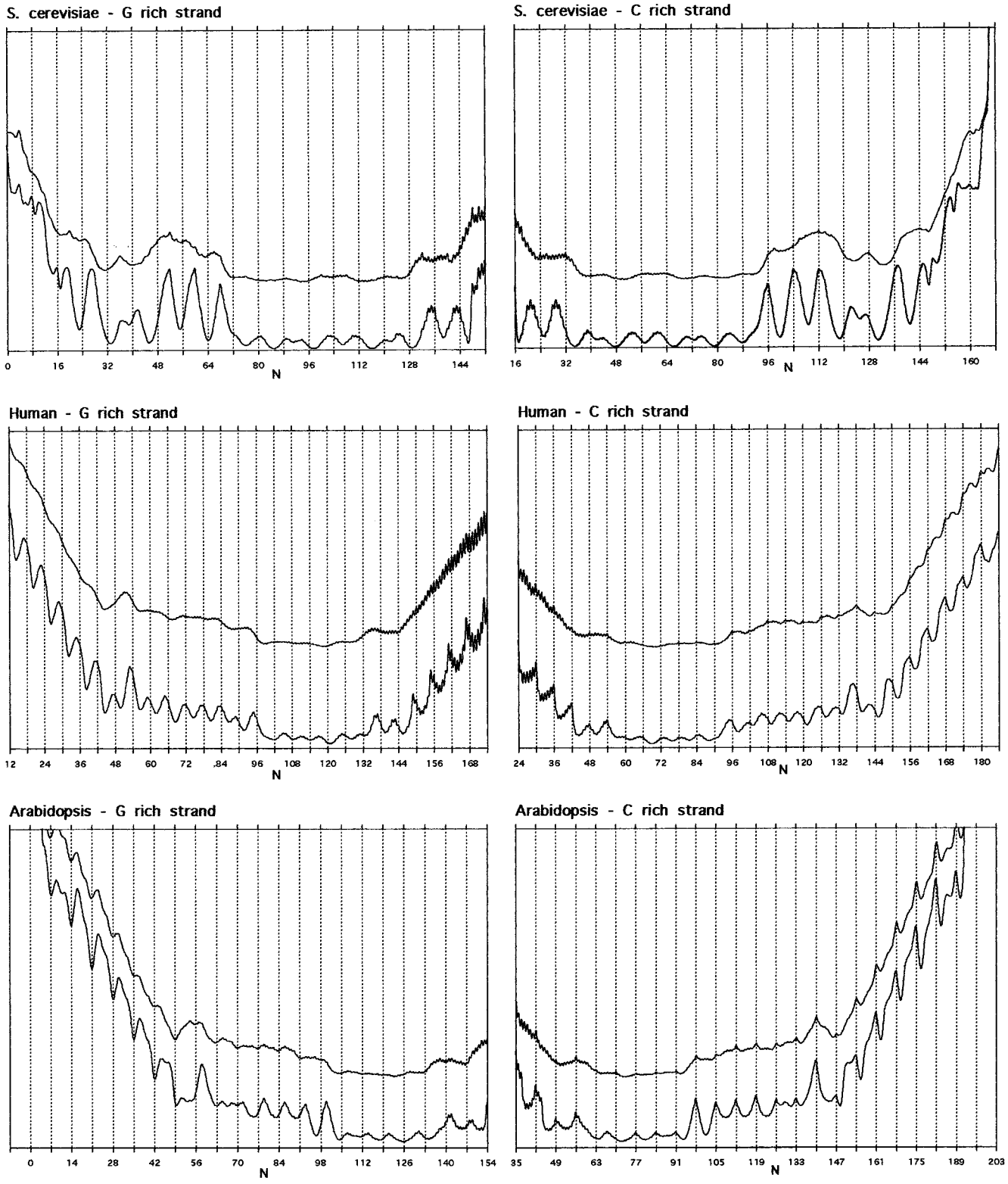

FIGURE 4: Theoretical simulation of DNase I footprinting. Each panel reports the simulation of DNase I cutting hypothesizing translational positions differing by 1 bp (upper profile) or by a number of bp equal to the telomeric repeat (lower profile).

nucleosome positioning with a spacing equal to the telomere repeat.

DISCUSSION

It is now generally recognized that DNA sequences play an essential role in determining intrinsic and/or induced curvature of the axis of the double helix in the B conformation (*13*, *27*). DNA flexibility appears particularly relevant in determining the energy cost of DNA wrapping around the histone octamer (*16*, *23*) and in nucleosome translational and rotational positioning along different DNA sequences (*13*). While the rules of nucleosome translational positioning are not yet fully clarified, the energy spent in bending DNA around the histone octamer to form nucleosomes and the ability of the histone octamer to interact preferentially with the same side of the B DNA double helix seem to depend

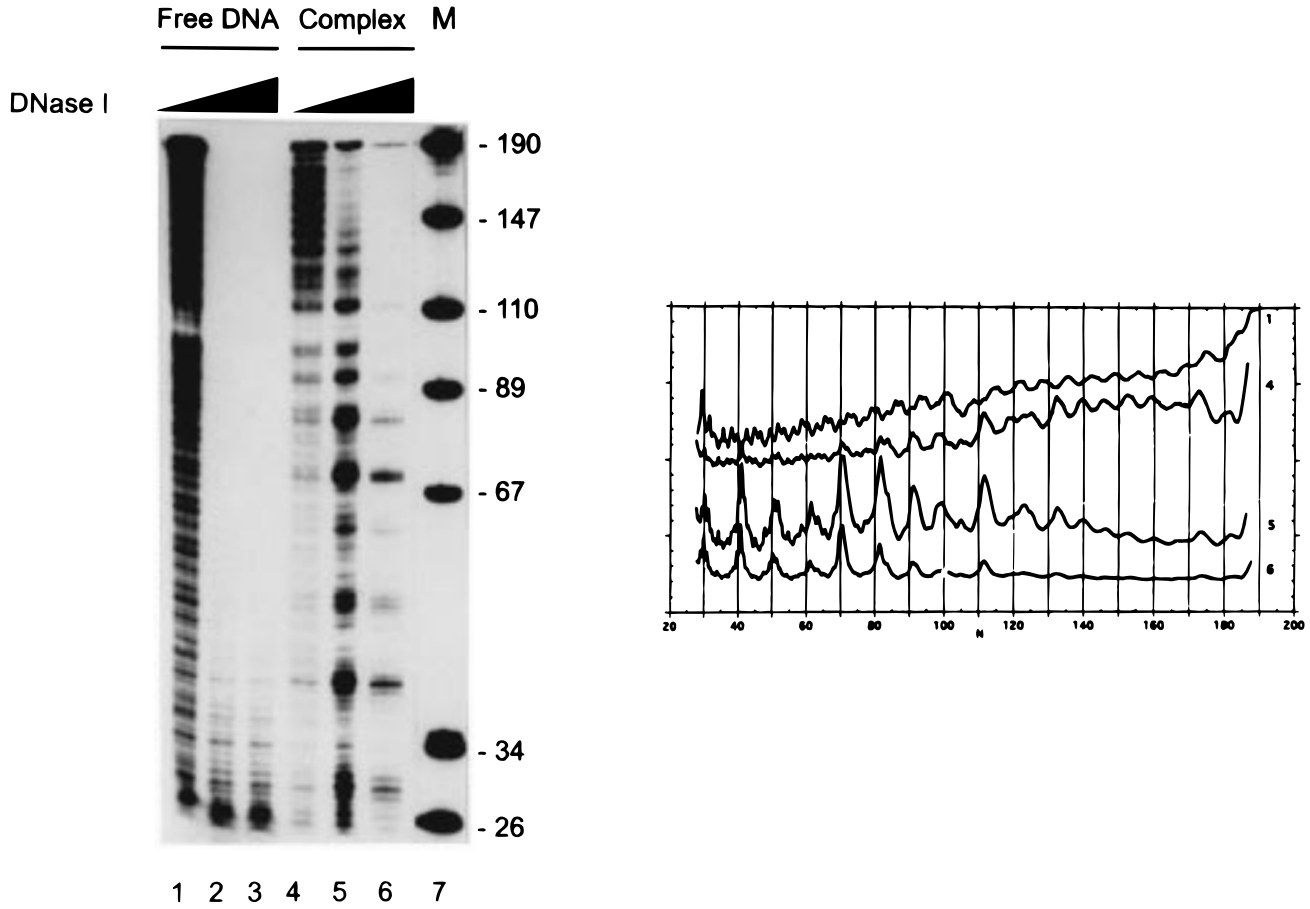

FIGURE 5: Nucleosomal DNA helical repeat derived from DNase I digestion of internally labeled *Arabidopsis* telomeric DNA. Left: DNase I footprinting at increasing enzyme amounts: (free DNA) lane 1, 10 U/mL DNase I; lane 2, 50 U/mL; lane 3, 100 U/mL; (nucleosome) lane 4, 50 U/mL; lane 5, 250 U/mL; lane 6, 500 U/mL. M is a digest of pUC18 with *Hpa*II. Right: densitometric tracings of lane 1 (free DNA), and lanes 4, 5, and 6 (nucleosome).

strongly on the intrinsic capability of the DNA sequences to bend (*15*, *23*).

From these quite general considerations, it appears highly probable that, when the peculiar features of the DNA sequence make the axis of the double helix "straight", the energy cost of the DNA curvature and/or distortion around the histone octamer must be higher than in average DNA sequences. In the eukaryotic genome, telomeric sequences possess these characteristics. Most telomeres are characterized by a sequence periodicity (between 6 and 8 bp) lower than that of the B DNA double helix. A consequence of this phase difference should be lower association constants for telomeric nucleosomes with respect to average nucleosomes.

Our results confirm this hypothesis. In Table 1 we have compared the relative free energies of nucleosome formation obtained for telomeric sequences with those for sequences from other laboratories, namely repetitive DNAs associated with some genetic diseases (*42*), pericentromeric DNAs in mouse (*25*), *X. borealis* 5S RNA gene (*42*, *43*), and TG repeats (*23*). Telomeric sequences are the only ones characterized by a positive $\Delta\Delta G$ with respect to average nucleosomal DNA. According to the Boltzmann equation, the differences in the binding affinity for the histone octamer of telomeric DNAs with respect to the average sequence DNA would be 5−15-fold at room temperature, whereas considering the most favored nucleosome positions along a genome, the difference can be evaluated at about 100−1000-fold. It is intriguing to suggest that, while the bulk of the eukaryotic genome seems to not be constrained or evolved to aid nucleosome organization, as shown by Lowary and Widom (*44*), DNA flexibility could remarkably contribute to the structural organization of telomeric chromatin domains. It is worth considering that even if positive free-energy values of telomeric nucleosomes were expected, this is not true for every straight DNA. Sinden and cow (*28*) showed that DNA fragments containing CTG triplet repeats derived from the human myotonic dystrophy gene migrate up to 20% faster than expected in nondenaturing gels and suggested that the results can be explained by a 20% increase in persistence length of the DNA. Therefore, these sequences can be considered the straightest among the natural sequences so far assayed. Surprisingly, Wang and Griffith (*45*) and Godde and Wolffe (*42*) recently showed that CTG repeated sequences efficiently wrap around the histone octamer (see Table 1). Godde and Wolffe suggest that the high affinity for the histone octamer of CTG repeated sequences could derive from a preferred association with histones at the nucleosomal dyad. On the contrary, in the case of telomeric sequences, DNA flexibility is likely to play a dominant role with respect to other parameters in determining the free energy of nucleosome formation. Even though the number of telomeric sequences so far examined is too small to try to develop a general model, we can do some consideration. The telomeric sequences examined (Table 1) differ in their repeat length but are characterized by the conservation of

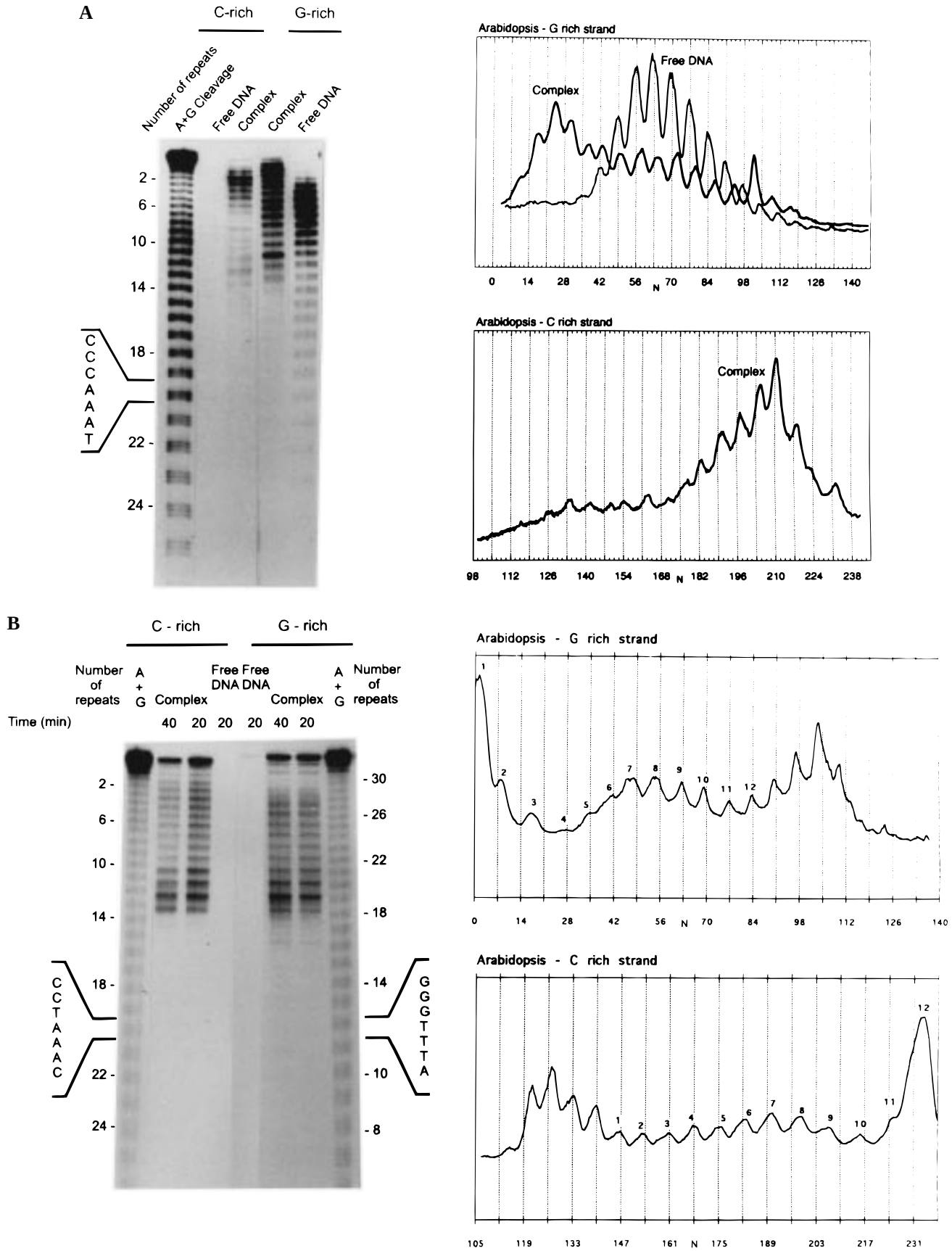

FIGURE 6: (A) Left: Exo III digestion of nucleosome reconstituted onto a 240-bp *Arabidopsis* telomeric DNA. Right: densitometric profiles. (B) λ exonuclease footprinting of the same sequence. Bands corresponding to the borders of the same nucleosome have been labeled with the same number.

short sequence motifs such as GGG and TGG. These two trinucleotides were shown to have a nonrandom positioning in chicken erythrocyte nucleosomes, since they preferentially face outside with respect to the histone octamer (*14*). On

account of telomeric repeat lengths, this orientation is not allowed at every DNA turn in telomeric nucleosomes and this should increase the energy required for wrapping around the histone octamer.

Our footprinting studies put interesting structural details in evidence. All of our experiments show that telomeric nucleosomes occupy multiple translational positions without a preferred rotational setting. However, the structure of the individual nucleosome is not altered, since a prolonged digestion with DNase I revealed the canonical nucleosomal DNA periodicity of 10.2 bp. Furthermore, DNase I cleavage theoretical simulation and Exo III and λ exonuclease footprintings allow one to distinguish between two possible models of multiple nucleosome positioning. In the first model, nucleosome positions differ by one base pair, because of the lack of local chemical recognition between the histone octamer and the DNA bases; according to the second model, nucleosome-preferred positions are spaced by the number of base pairs equal to the telomere repeat, indicating that local chemical recognition could play an important role in nucleosome positioning. The results reported in this paper strongly support the second model and are in agreement with the recently resolved structure of the nucleosome at 2.8 Å which reveals a relevant role of local chemical interactions in nucleosome assembly (*33*).

Mapping of nucleosomes formed onto telomeric sequences may give a useful insight both on the role of repetitive DNA sequences in nucleosome organization and on peculiar features such as lower thermodynamic stability and high mobility of telomeric nucleosomes. Interesting structural features could emerge from studies on different telomeric sequences with the same repetition period that are now in progress in our laboratory. An example is *Tetrahymena* telomeric DNA $(TTGGGG)_n$, which has the same 6-bp repeat length as that of human but is characterized by a 4-G stretch, and it shows the lowest association constant with the histone octamer between telomeric sequences so far studied (*16*).

ACKNOWLEDGMENT

Thanks are due to P. De Santis for many helpful discussions, to R. Negri and M. Buttinelli for kindly sharing with us their method of nucleosome mapping by λ exonuclease and for useful advice in hydroxyl radical footprinting, and to M. Longo for preliminary experiments.

REFERENCES

1. Zakian, V. A. (1995) *Science 270*, 1601−1607.
2. Greider, C. W. (1996) *Annu. Rev. Biochem. 65*, 337−365.
3. Williamson, J. R. (1994) *Annu. Rev. Biophys. Biomol. Struct. 23*, 703−730.
4. Rhodes, D., and Giraldo, R. (1995) *Curr. Opin. Struct. Biol. 5*, 311−322.
5. Kang, C. H., Berger, I., Locksin, C., Ratliff, R., Moyzis, R., and Rich, A. (1994) *Proc. Natl. Acad. Sci. U.S.A. 91*, 11636−11640.
6. König, P., Giraldo, R., Chapman, L., and Rhodes, D. (1996) *Cell 85*, 125−136.
7. Makarov, V. L., Lejnine, V. L., Bedoyan, J., and Langmore, J. P. (1993) *Cell 73*, 775−787.
8. Tommerup, H., Dousmanis, A., and de Lange, T. (1994) *Mol. Cell. Biol. 14*, 5777−5785.
9. Lejnine, V. L., Makarov, V. L., and Langmore, J. P. (1995) *Proc. Natl. Acad. Sci. U.S.A. 92*, 2393−2397.
10. Fajkus, J., Kovarik, A., Kralovics, R., and Bezdek, M. (1995) *Mol. Gen. Genet. 247*, 633−638.
11. Bedoyan, J., Lejnine, V. L., Makarov, V. L., and Langmore, J. P. (1996) *J. Biol. Chem. 271*, 18485−18493.
12. Muyldermans, S., DeJonge, J., Wyns, L., and Travers, A. A. (1994) *Nucleic Acids Res. 22*, 5635−5639.
13. Travers, A. A. (1987) *Trends Biochem. Sci. 12*, 108−112.
14. Satchwell, S. C., Drew, H. R., and Travers, A. A. (1986) *J. Mol. Biol. 216*, 69−84.
15. Shrader, T. E., and Crothers, D. M. (1990) *J. Mol. Biol. 216*, 69−84.
16. Cacchione, S., Cerone, M. A., and Savino, M. (1997) *FEBS Lett. 400*, 37−41.
17. Alessi, R., Cacchione, S., De Santis, P., Fuà, M., and Savino, M. (1997) *Biophys. Chem. 67*, 151−158.
18. Razvi, F., Gargiulo, G., and Worcel, A. (1983) *Gene 23*, 175−183.
19. Drew, H. R., and Travers, A. A. (1985) *J. Mol. Biol. 186*, 773−790.
20. Rhodes, D., and Laskey, R. A. (1989) *Methods Enzymol. 170*, 575−585.
21. Forte, P., Leoni, L., Sampaolese, B., and Savino, M. (1989) *Nucleic Acids Res. 17*, 8683−8694.
22. Tullius, T. D., Dombroski, B. A., Churchill, M. E. A., and Kam, L. (1987) *Methods Enzymol. 155*, 537−558.
23. Shrader, T. E., and Crothers, D. M. (1989) *Proc. Natl. Acad. Sci. U.S.A. 86*, 7418−7422.
24. Jayasena, S. D., and Behe, M. J. (1989) *J. Mol. Biol. 208*, 297−306.
25. Widlund, H. R., Cao, H., Simonsson, S., Magnusson, E., Simonsson, T., Nielsen, P. E., Kahn, J. D., Crothers, D. M., and Kubista, M. (1997) *J. Mol. Biol. 267*, 807−817.
26. Hayes, J. J., Bashkin, J., Tullius, T. D., and Wollfe, A. P. (1991) *Biochemistry 30*, 8434−8440.
27. Hagerman, P. (1990) *Annu. Rev. Biochem. 59*, 755−781.
28. Chastain, P. D., II, Eichler, E. E., Kang, S., Nelson, D. L., Levene, S. D., and Sinden R. R. (1995) *Biochemistry 34*, 16125−16131.
29. Cacchione, S., De Santis, P., Foti, D., Palleschi, A., and Savino, M. (1989) *Biochemistry 28*, 8706−8713.
30. Klug, A. A., and Lutter, L. C. (1981) *Nucleic Acids Res. 9*, 4267−4283.
31. Price, M. A., and Tullius, T. D. (1992) *Methods Enzymol. 212*, 194−219.
32. Michalik, V., Spotheim Maurizot, M., and Charlier, M. (1995) *J. Biomol. Struct. Dyn. 13*, 565−575.
33. Luger, K., Mäder, A. W., Richmond, R. K., Sargent, D. F., and Richmond, T. J. (1997) *Nature 389*, 251−260.
34. Lutter, L. C. (1978) *J. Mol. Biol. 124*, 391−420.
35. Buttinelli, M., Di Mauro, E., and Negri, R. (1993) *Proc. Natl. Acad. Sci. U.S.A. 90*, 9315−9319.
36. Cacchione, S., Cerone, M. A., De Santis, P., and Savino, M. (1995) *Biophys. Chem. 53*, 267−281.
37. Linxweiler, W., and Horz, W. (1982) *Nucleic Acids Res. 10*, 4845−4859.
38. Thomas, K. R., and Olivera, B. M. (1978) *J. Biol. Chem. 253*, 424−429.
39. Camier, S., Gabrielsen, O., Baker, R., and Sentenac, A. (1985) *EMBO J. 4*, 491−500.
40. Mymryk, J. S., and Archer, T. K. (1994) *Nucleic Acids Res. 22*, 4344−4345.
41. Flaus, A., Luger, K., Tan, S., and Richmond, T. J. (1996) *Proc. Natl. Acad. Sci. U.S.A. 93*, 1370−1375.
42. Godde, J. S., and Wolffe, A. P. (1996) *J. Biol. Chem. 271*, 15222−15229.
43. Schild, C., Claret, F.-X., Wahli, W., and Wolffe, A. P. (1993) *EMBO J. 12*, 423−433.
44. Lowary, P. T., and Widom, J. (1997) *Proc. Natl. Acad. Sci. U.S.A. 94*, 1183−1188.
45. Wang, Y.-H., and Griffith, J. (1995) *Genomics 25*, 570−573.

BI9726180